Journal of Magnetism and Magnetic Materials 324 (2012) 2342–2348

Contents lists available at SciVerse ScienceDirect

Journal of Magnetism and Magnetic Materials

journal homepage: www.elsevier.com/locate/jmmm

Magnetic behavior of a nano-disk constrained in an antiferromagnetic substrate

J.C.S. Rocha [a], B.V. Costa [a], P.Z. Coura [b,*], S.A. Leonel [b], R.A. Dias [b]

[a] Departamento de Física, Laboratório de Simulação, ICEX, UFMG, 30123-970 Belo Horizonte, MG, Brazil
[b] Departamento de Física, ICE, UFJF, 36036-330 Juiz de Fora, MG , Brazil

ARTICLE INFO

Article history:
Received 24 November 2011
Received in revised form
6 February 2012
Available online 23 February 2012

Keywords:
Exchange bias
Magnetic nano-disk
Monte Carlo
Heisenberg
Dipolar interaction

ABSTRACT

In this work we report a numerical Monte Carlo study of the behavior of a magnetic nano-disk put over an antiferromagnetic substrate. Three approaches were considered for describe the substrate: (1) A stacked antiferromagnetic configuration, (2) an Ising like arrangement and (3) Heisenberg like spins. For the Heisenberg case we still have considered an easy-plane and an easy-axis symmetry of the substrate. The hysteresis loop for the nano-disk is obtained by considering the three cases. The signature of the vortex in the nano-disk appears as small jumps in the hysteresis curve. Exchange bias effects are observed since the substrate has an easy axis symmetry.

1. Introduction

Magnetic devices have many applications in technology, for example in magnetic random access memories (MRAMSs), digital reading heads, position sensors, amperimeters and several others [1,2]. It is possible that many new applications will be discovered in the next few years. An important issue in digital recording is the density of information that can be stored in a device. Several technological advances have pushed this limit forward since the 10^5 bit/inch density in the 1970 decade up to 10^9 bit/inch nowadays. The future of the high density recording devices will depend of our capacity to develop more sensitive sensors and materials capable of overcome the super-paramagnetic limit [3,4]. That is a natural limit imposed by thermal fluctuations which determines how long the magnetization of a ferromagnetic structure survives, or in other words: The long-range ferromagnetic order vanishes when the energy due to the anisotropy becomes comparable to thermal fluctuation energy [5,6]. Some properties of nano-magnets can help to overcome the super-paramagnetic limit by allowing to create new mechanisms for building sub-micron magnetic devices [7–9]. One of the most promising candidates is a vortex structure [10–15] that can develop in quasi-two-dimensional nano-magnetic systems [16–18]. By a vortex we mean a special configuration of spins similar to the stream lines of a circulating flow in a fluid. The magnetic moments precess by 2π on a closed path around the vortex. In a finite system the competition between the magnetostatic energy and the exchange interaction is responsible for the formation of a magnetic vortex [19–21]. The surface effects influence the magnetic properties [22] in such a way that they become increasingly important as the particle size decreases [23]. Instead of an ordered ferromagnetic configuration the ground state of a nano-disk can be a single vortex or a capacitor-like state [20,21]. In Fig. 1 we show a schematic view of these configurations. The behavior of a magnetic material in the presence of an external magnetic field is described by its hysteresis curve. One of the most interesting properties is the remanent magnetization which is a residual magnetization in the material when the aligning field is reduced to zero. Of interest are also the coercive and the saturation fields. They are the fields required for canceling the residual magnetization and the field required for forcing all magnetic moments of the sample to point in the direction of the field respectively. In 1956 Meiklejonh and Bean [24] reported that partially oxidized *Co* fine particles exhibited hysteresis loops displaced along the magnetic field axis. Not long after that they recognized this behavior was due to exchange coupling between ferromagnetic (F) and antiferromagnetic (AFM) layers [25]. This phenomenon is known as exchange bias (EB) effect. The shift is attributed to the frozen-in global unidirectional anisotropy of the system [26–29]. Since its discovery, the EB effect has been observed in several different materials [30–35]. Magnetic coupling of FM nano-particles with an AFM matrix shown to improve the thermal stability of magnetization of the FM nano-particles [4]. Therefore,

* Corresponding author.
E-mail addresses: jcsrocha@fisica.ufmg.br (J.C.S. Rocha), bvc@fisica.ufmg.br (B.V. Costa), pablo@fisica.ufjf.br (P.Z. Coura), sidiney@fisica.ufjf.br (S.A. Leonel), radias@fisica.ufjf.br (R.A. Dias).

0304-8853/$ - see front matter © 2012 Published by Elsevier B.V.
doi:10.1016/j.jmmm.2012.02.028

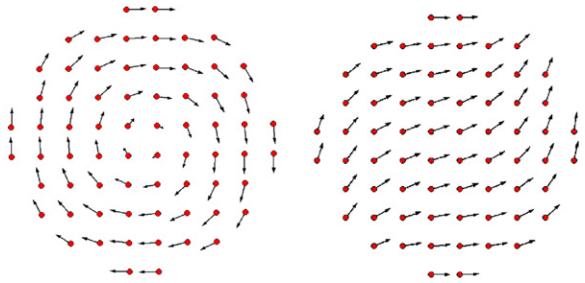

Fig. 1. Schematic view of two possible spins configurations on a ferromagnetic nano-disk: a vortex (left hand side) and a capacitor-like state (right hand side).

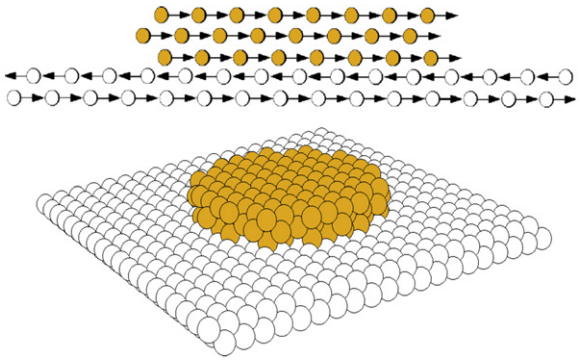

Fig. 2. This figure shows our simulation setup. The figure at the top is a side view evidencing the antiferromagnetic spin configuration in the substrate. The figure at the bottom is a perspective view of the nano-particle over the substrate not showing the magnetic moments. The nano-disk is put over the (100) face of the substrate. Interactions between the nano-disk and the substrate consider only first neighbors. The *XY* plane is the plane of the substrate. These spins configuration is called of the uncompensated spins.

it allow magnetically stable dots only a few nano-meters in size, which would surpass the storage-density as set by the magnetic-storage industry [4].

In this work we use Monte Carlo and spin dynamics to study the EB effect in FM nano-disks settled over AFM substrates (The arrangement is shown in Fig. 2.). The hysteresis loop is obtained by considering three different arrangements of the spins in the substrate: frozen, Ising like and classical Heisenberg. Those choices will be made clearer in the following. The signature of the vortex in the nano-disk appears as small jumps in the hysteresis curve. The exchange bias is observed since that the substrate has an easy axis symmetry, in others words, the substrate has a preferential direction which can be build by introducing an anisotropy in a given direction.

2. Model

Theoretically we can consider a pseudo-spin Hamiltonian model to describe a magnetic nano-disk as [36–41]

$$H_{disk} = -J\sum_{\langle i,j\rangle}\vec{S}_i\cdot\vec{S}_j - B\sum_i S_i^x + D\sum_{i\neq j}\left[\frac{\vec{S}_i\cdot\vec{S}_j}{r_{ij}^3} - \frac{3(\vec{S}_i\cdot\vec{r}_{ij})(\vec{S}_j\cdot\vec{r}_{ij})}{r_{ij}^5}\right], \quad (1)$$

where $J>0$ is an exchange interaction constant coupling spins $\vec{S}_i$ and $\vec{S}_j$ at sites i and j and $r_{i,j}$ is the distance between sites at positions i and j. B is an external magnetic field in the x direction and D is the strength of a dipole–dipole interaction. For the dipole

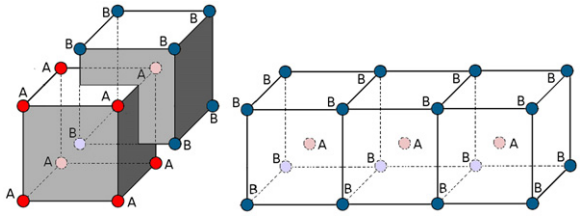

Fig. 3. The left figure show BCC lattice as interlaced SC lattices and the right show as structure of alternating layers.

interaction we have fixed $D/JS^2 = 0.2$. The sum in the first term runs over first neighbors, in the second and third terms is over the entire lattice [21,42]. In this work, when not explicitly defined, energy and temperature will be given in units of JS^2 and k_b/JS^2 respectively. Here k_B is the Boltzmann constant. The physics behind Hamiltonian (1) can be understood as follows. The exchange interaction forces the magnetic moments of neighboring sites to point in the same direction. The dipole interaction is divided into two terms: $([\vec{S}_i\cdot\vec{S}_j]/r_{ij}^3)$ tends to align the magnetic moments anti-ferromagnetically since $D>0$. The term $(-3[(\vec{S}_i\cdot\vec{r}_{ij})(\vec{S}_j\cdot\vec{r}_{ij})]/r_{ij}^5)$ aligns the magnetic moments along the direction of the unit vector $\hat{r}_{ij}$. The nano-disk vortex configuration sets a balance that meets the requirement to minimize the energy. The magnetic moments along the border are aligned along the vector that unites them, satisfying the condition to minimize the second term of the dipole and exchange interactions. In the following sections we will use numerical Monte Carlo and spin dynamics simulation to study the magnetic behavior of a FM nano-disk over a AFM substrate. As a matter of comparison we consider firstly the magnetic behavior of the nano-disk over a paramagnetic (PM) substrate. The hysteresis loop depends on the nano-disk ground state. In a nano-disk which has a vortex configuration as ground state presents a typical loop as be seen in Fig. 4. The vortex signature is seen as the small steps in the hysteresis curves. The remanent magnetization is zero. The zero remanent magnetization is due the null magnetization of the vortex configuration. The steps in the hysteresis curves appear as a consequence of the pinning of the vortex at the lattice sites. When the external magnetic field is turned on the vortex in the nano-disk start to move in a direction perpendicular to the field. The vortex displacement direction depends on its curl direction (see Fig. 5). Due to this dependence and the linearity with the field strength we can say that a force acting on the vortex core is $\vec{F}\propto\vec{q}\times\vec{B}$. Where $\vec{q}=\pm\hat{z}$ for counter clockwise or clockwise vortex curl direction respectively. Therefore, measurements of the vortex displacement can determine the vortex chirality. The vortex energy is smaller when its center coincides with the center of a plaquette that is formed by four sites in a square lattice (see Fig. 3). To move from one site to another the magnetic field has to be augmented so that the vortex can overcome through the pinning barrier. By considering that the vortex is at the center of a plaquette we can estimate the steps on the hysteresis loop by calculating the gain in magnetization when the vortex moves for a lattice spacing. For an object in the form of a nano-disk we obtain

$$\Delta m_x = \frac{2\sqrt{2}}{\pi}\frac{1}{L}\approx\frac{0.900}{L}. \quad (2)$$

If we consider squared nano-particle we should obtain $\Delta m_x = L^{-1}$, where L is the particle diameter. For $L=10$ and $L=20$ Eq. (2) gives $\Delta m_x\approx 0.090$ and 0.045 respectively. In our simulations we have measured $\Delta m_x = 0.130$ and 0.065 in both cases. Those results are

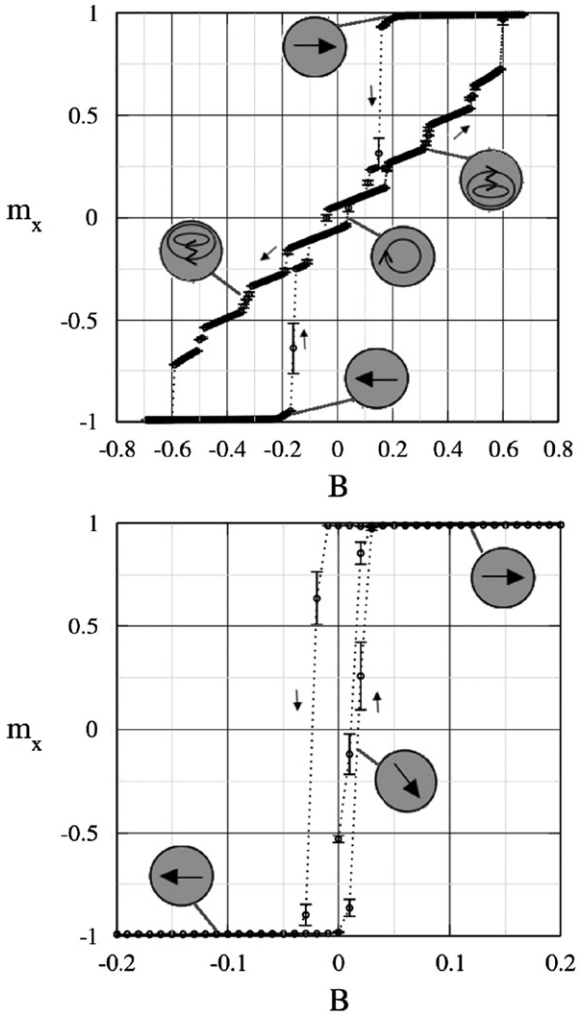

Fig. 4. The figure at the top show a hysteresis loop for a nano-disk which has a vortex as ground state and the figure at the bottom show the loop when nano-disk present a capacitor as ground state.

qualitatively in agreement with the estimates, indicating that the pining should disappear in the thermodynamic limit ($L\to\infty$).

The EB phenomena can be described in terms of the substrate spin alignment at the interface [29]. Concerning the orientation of the spins at the interface the surface can be compensated or uncompensated AFM. Experimentally the main problem in the study of such phenomenon is the difficulty to determine the exact spin configuration at the interface. It is customary to assume that the bulk spin configuration is preserved although it is possible that at the interface the AFM atoms relax or reconstruct. In a compensated AFM interface the net spin averaged over a macroscopic length scale is zero. Therefore, this kind of surface will have zero net magnetization. In contrast, if the spin arrangement is such that the surface magnetization is non-zero, the surface is uncompensated [43–45]. We consider the nano-disk and the substrate as having a body centered cubic (BCC) structure. The setup for our simulation is shown in Fig. 2. The nano-disk is put epitaxially over the (100) face of the BCC substrate. The BCC lattice can be seen as two interlaced simple cubic (SC) lattices as seen in Fig. 3. The linear size of the substrate is chosen such that $L_s = 2L$. Periodic boundary conditions are assumed in the X and Y directions.

The total Hamiltonian describing the system is

$$H_{total} = H_{disk} - J_{d-s}\sum_{inter}\vec{S}_i\cdot\vec{s_j} + J_s\sum_{sub}\vec{s}_i\cdot\vec{s_j} - B\sum_{sub}s_i^x. \quad (3)$$

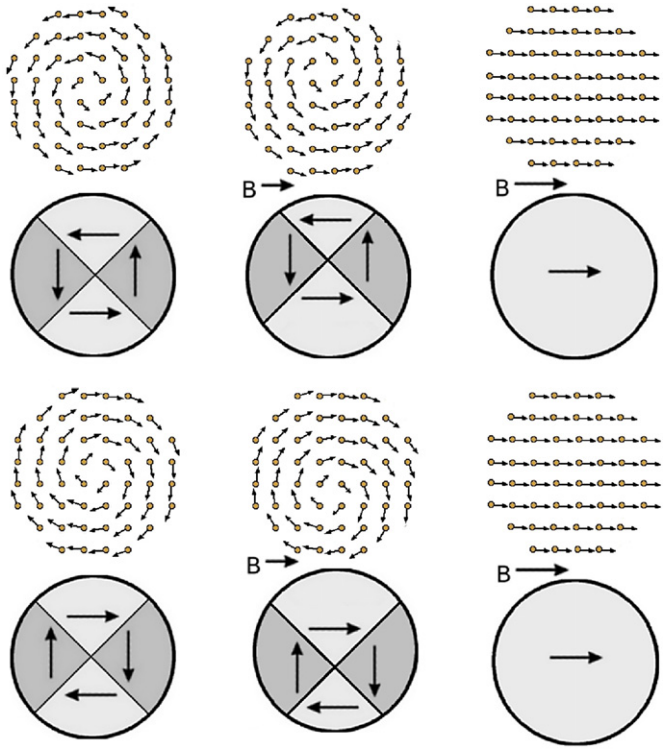

Fig. 5. Schematic representation of the path followed by the vortex under the action of an external magnetic field. Top and bottom figures are for counter clockwise and clockwise vortex curl directions respectively.

The spin variables $\vec{S}_i$ and $\vec{s}_i$ refer to the nano-disk and substrate respectively. The first sum is to be performed over the nearest neighbors sites between the nano-disk and the substrate at the interface, the second sum is performed over the nearest neighbors sites in the substrate where $J_s > 0$ is the exchange interaction constant coupling spins $\vec{s}_i$ and $\vec{s}_j$, finally the third sum is over all sites in the substrate. Both values J and J_s can be experimentally determined and $J > J_s$ [28]. However, the value of the exchange bias field depends on the unknown parameter J_{d-s} that cannot be experimentally determined and in this work we set $0 < J_{d-s} \le J_s$.

3. Substrate models and results

The numerical calculation is done as follows. The substrate and the nano-disk initial configurations are chosen at random and the particle diameter depends on condition given by Eq. (4). The external magnetic field is turned on at time $t=0$ and applied in the x direction. We note that *time* unity is to be understood as a Monte Carlo step (MC step). The magnetic field is increased or decreased in steps of size $\Delta B = 0.01$ measured in unities of $JS/g\mu_B$, where g is the Landè factor and μ_B is the Bohr's magneton. For each value of the magnetic field 10^3 time steps are performed in order to equilibrate the system. When saturation is reached in one direction the magnetic field is increased or decreased until the system saturates in the inverse direction. We use in this work three different types of model to simulate the substrates: (A) frozen spins, (B) Ising spins and (C) classical Heisenberg spins. They are defined as follows.

3.1. Frozen

For the frozen substrate we consider that the classical spin components are $s_i^y = s_i^z = 0$, and $s_i^x = +1$. We chose an

antiferromagnetic stacked configuration for the substrate, so that, it has no dynamics at all. The sum over the substrate becomes a constant and can be dropped out of H_{total}. The term summing over the interface can be seen as a local magnetic field acting in the $+x$ direction, introducing an preferential direction in the system. Thus, the interaction between nano-disk and the substrate can be replaced by an effective field, $B_{eff} = 4J_{d-s}$ like a Zeeman interaction applied on the first layer of the nano-disk. As should be expected the system exhibit the EB effect as shown in Fig. 6 for two values of the exchange constant J_{d-s}. Increasing J_{d-s} implies in an increasing of the EB effect.

3.2. Ising

An Ising-like substrate is built by choosing the spins components as $s_i^y = s_i^z = 0$ and $s_i^x = \pm 1$. This can be achieved by introducing a strong anisotropy in the x direction in the substrate. The scheme is shown in Fig. 7. Two different configurations are possible depending on the thickness, L_z^s, of the substrate and the nano-disk substrate interaction J_{d-s}. For low values of L_z^s one observe that a nano-disk domain is imprinted in the substrate [46]. A cylindrical region beneath the nano-disk will have its magnetization inverted, following the nano-disk magnetization. Therefore, the EB effect is not present. By energy considerations one can show that if L_z^s obey the condition

$$\frac{L_z^s}{L} > \frac{J_{d-s}}{4J_s}, \tag{4}$$

the substrate interface is completely uncompensated and therefore, the EB effect is observed. In the Fig. 8 the hysteresis loop for two systems fulfilling this condition is shown.

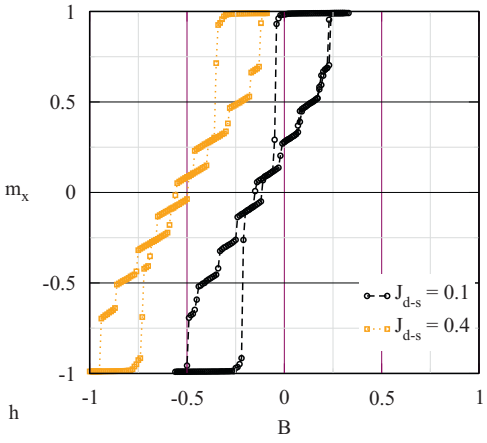

Fig. 6. The hysteresis loop is shown for the frozen substrate to two values of the exchange constant J_{d-s} and J_s=0.5.

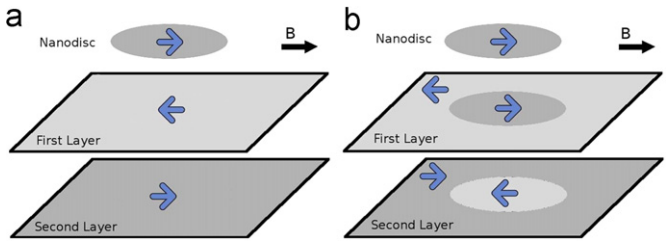

Fig. 7. Schematic representation of the configuration of the first two layers of spins for the Ising substrate. An external field, $\vec{B}$, is applied in the x direction. The difference in energy of configurations (a) and (b) shows that the (b) configuration is more stable.

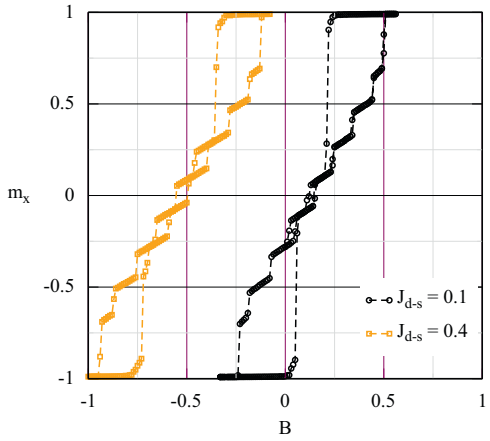

Fig. 8. Hysteresis loops for the Ising substrate using two values of the exchange constant J_{d-s}. In both cases $L_z^s/L > J_{d-s}/4J_s$. We use $L_z^s = 2$, D=0.2 and J_s=0.5. The values for J_{d-s} are shown in the insets. We use L=10 and L=20. If $L_z^s/L < J_{d-s}/4J_s$ (not shown) the exchange Bias effect is not observed.

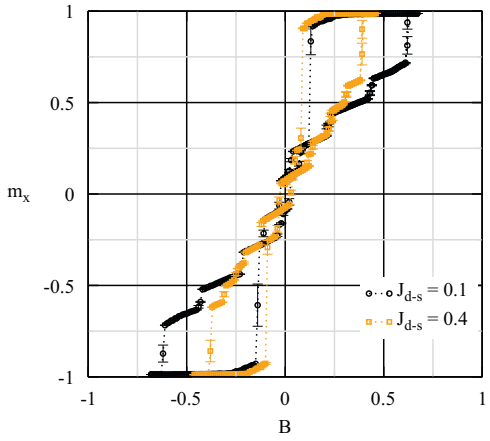

Fig. 9. Hysteresis loop when the substrate has an easy plane anisotropy. The signature of the presence of the vortex in the nano-disk is evidenced by the jump in the hysteresis loop [47]. Here J_s=0.5. We observe that the EB effect is not present for the chosen values of J_{d-s}. This should be expected since the vortex is imprinted in the substrate becoming an uncompensated structure.

3.3. Heisenberg

For the Heisenberg substrate we consider the classical spin vector as $\vec{s}_i = (s_i^x, s_i^y, s_i^z)$ satisfying the condition $|\vec{s}_i| = 1$. Due to the continuous degrees of freedom of $\vec{s}_n$ we get a richer structure than in both earlier cases. We will consider here the situations where the substrate has two different symmetries (1) an easy plane (EP) or (2) an easy axis (EA).

3.3.1. Easy plane symmetry

The easy plane model means that the spins in the substrate lower their energy by lying in the XY plane. In order to reach this condition we introduce a quadratic anisotropy in the z direction, so that, the Hamiltonian for such model is written as $H_{in-plane} = H_{total} + A\sum_{sub}(s_i^z)^2$ with $A > 0$. In this work we use $A/J = 1.0$. The EB effect is not expected to appears in the EP model since the substrate has no preferential direction of magnetization for B=0. Fig. 9 shows that there is no shift in the hysteresis loop as a function of the interface exchange interaction. Fig. 10 shows a schematic representation of the path followed by the magnetization with an easy-plane substrate. We observe that if the interface interaction is

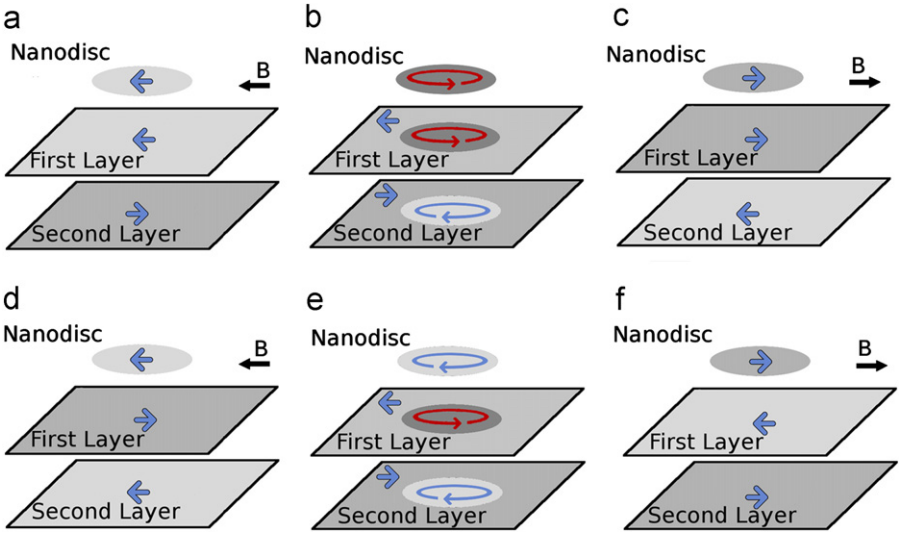

Fig. 10. Schematic representation of the path followed by the magnetization with an easy-plane substrate. Top and bottom figures are for ferro and anti-ferromagnetic coupling, respectively. In any case the vortex is imprinted in all layers of the substrate.

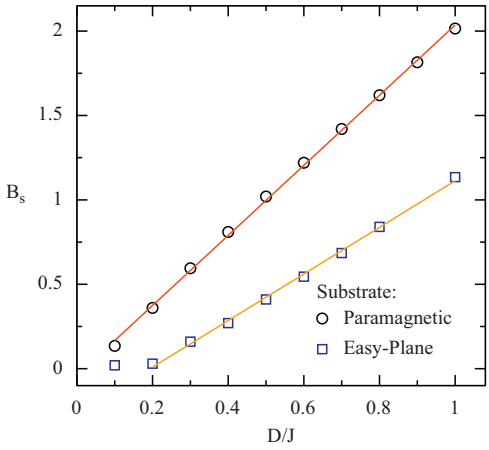

Fig. 11. Saturation field in function of dipolar strength of nano-disks deposited over PM and AFM substrates.

ferromagnetic or anti-ferromagnetic the vortex in the first layer in the substrate will appears in the same or opposite direction according with the magnetization of the nano-disk. In Fig. 10, from left to right, the nano-disk is initially saturated in the $-x$ direction. As the external field is augmented a vortex appears in the nano-disk. For strong enough interaction (J_{d-s}) the vortex is imprinted in the surface propagating to all layers down in the substrate. The AF substrate has the property to reduce the nano-disk saturation field. We can though the substrate as an effective field added to the external applied field it will increase the interaction at the interface implying in a decrease of the field necessary to saturate the nano-disk (see Fig. 9). In Fig. 11 we compare the saturation field between nano-disks deposited over PM and AFM substrates. A plot of the saturation field as a function of the dipole strength interaction shows a linear behavior as seen in Fig. 11.

3.3.2. Easy axis substrate

A substrate with an easy axis can be built by introducing an anisotropy in the x direction. In this case the Hamiltonian for the system is written as $H_{easy-axis} = H_{total} - A\sum_{sub}(S_i^x)^2$. The spins in the substrate have a $\mathbb{Z}_2$ symmetry [48,49], so that, it should behave as an Ising system in the x direction for A greater than zero. It is easy

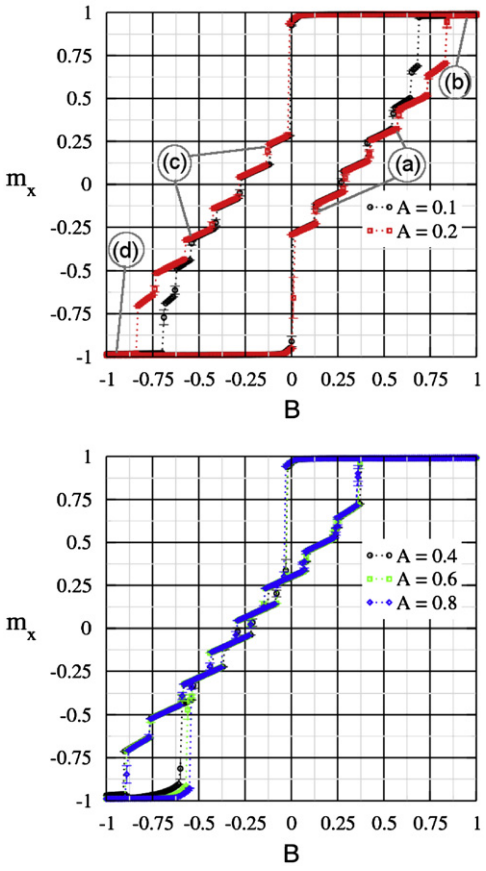

Fig. 12. Hysteresis loop for several anisotropy strength.

to see that the condition

$$A > \frac{\pi J_{d-s}}{4L_z^s} \tag{5}$$

has to be fulfilled in order to the EB effect appears. At low values of A the *EB* effect does not appears, however, the hysteresis loop becomes larger with the saturation field increasing in both direction as seen in Fig. 12. On the other side, if the anisotropy is given by the condition in Eq. (5) the hysteresis shows the EB

effect as seen in Fig. 13. Beside the conditions for EB pointed above we must be sure that the substrate remains in an antiferromagnetic arrangement for any field value. For a fixed field this condition will depend on A and J_s. Now, by fixing the anisotropy, A, using the criterium stated in Eq. (5) we can find the behavior of the substrate configuration as a function of J_s. In Fig. 14 we show the B–J_s *phase diagram* for the easy axis case. We observe three possible configurations for the substrate: antiferromagnetic (AFM), spin flop (SF) and saturated (S). The boundaries of the diagram can be obtained by comparing the energy in the three different configurations and in our simulations we found that the point separating the three phases is $J_S^t = 0.59$. The maximum field applied B_{max} that does not change the state of the substrate (AF) to the saturated (S) or spin-flop (SP) phases is obtained as

$$B_{max} = \frac{K}{\mu_B g}\left(1-\frac{1}{L_z^s}\right), \tag{6}$$

where K is the exchange stiffness and can be written as

$$K = \frac{n_{vS} J_s S^2}{a}, \tag{7}$$

where n_{vS} is the number of first neighbors of the substrate, a is the lattice parameter and S the spin modulus. In this work we using

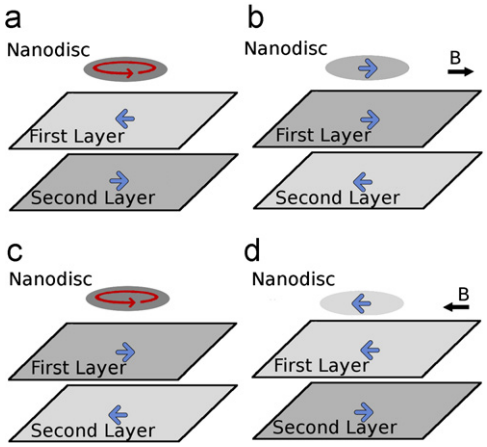

Fig. 13. Schematic representation of the path followed by the magnetization with an easy-axis substrate and low anisotropy constant. (a), (b), (c), and (d) positions at hysteresis loop are shown in Fig. 12.

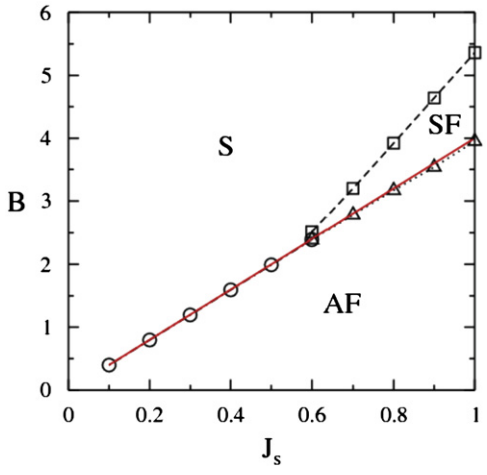

Fig. 14. Diagram showing the phases of the substrate, antiferromagnetic (AF), saturated (S) and spin-flop (SF) in function of J_s. The black lines with symbols correspond to simulation results and red lines without symbols the analytical results. We use $J_{d-s} = 0.1$.

$\mu_B = 1$, $g = 1$, $a = 1$ and $S = 1$, thus,

$$B_{max} = n_{vS} J_s \left(1-\frac{1}{L_z^s}\right). \tag{8}$$

In a BCC lattice, $n_{vS} = 8$, then

$$B_{max} = 8 J_s \left(1-\frac{1}{L_z^s}\right). \tag{9}$$

Finally to $L_z^s = 2$, we have

$$B_{max} = 4 J_s. \tag{10}$$

Our theoretical results agree with the simulation results as is shown in Fig. 14.

4. Final remarks, conclusions, and perspectives

We have used Monte Carlo simulations to study the magnetic behavior of a nano-disk put over an antiferromagnetic surface. Three different arrangements for the substrate were considered: (1) a stacked antiferromagnetic configuration, (2) an Ising like arrangement and (3) Heisenberg like spins. For the Heisenberg case we still considered an easy-plane and an easy-axis symmetry of the substrate. As expected the exchange bias effect appearing in the nano-disk depends on the symmetry of the substrate. In Fig. 15 we show a plot of the exchange bias field as a function of the interaction strength between the nano-disk and the substrate that resumes our results.

It is interesting to observe that the curves for the frozen, Ising and easy axis models coincide, inside the error bars. Using a linear regression we have obtained the exchange bias field B_{EB} as function of J_{d-s} for the three models as

$$B_{EB} = 1.300(1) J_{d-s} - 0.010(1). \tag{11}$$

This behavior does not dependent on the substrate thickness, L_z^s, since the condition (4) is satisfied. To a typical experimental value $J = 10$ meV the magnitude of the exchange bias field of our results is on the order of 10 Teslas. This value is greater than the experimental values by a factor 10 or more. We believe that this result is due to thickness of the nano-disk. Some preliminary results show that the B_{EB} decrease with increasing nano-disk thickness as in thin films [50]. This is probably due to the substrate effective field influence becomes smaller. However, more systematic simulations need to be carry out in order to get a quantitative understanding of that. Although B_{EB} does not depend on the easy axis anisotropy, A, since $A > A_{min}$, the hysteresis loop may present a deformation for high values of J_{d-s}.

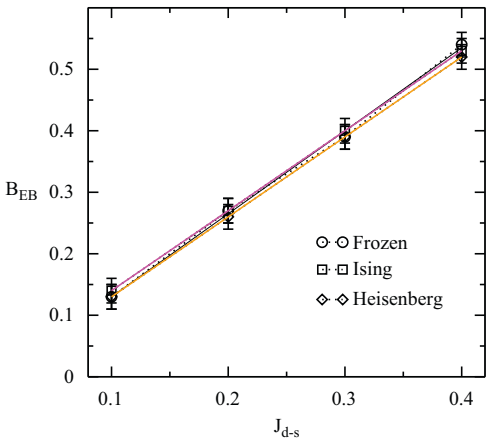

Fig. 15. Exchange bias for the three models: frozen, Ising and easy axis Heisenberg. We use $J_s = 0.5$.

Acknowledgments

This work was partially supported by CNPq and FAPEMIG (Brazilian Agencies).

References

[1] B. Heinrich, J.A.C. Bland, Ultrathin Magnetic Structures III—Fundamentals of Nanomagnetism, Springer, Berlin, Heidelberg, New York, 2005.
[2] B. Heinrich, J.A.C. Bland, Ultrathin Magnetic Structures IV—Applications of Nanomagnetism, Springer, Berlin, Heidelberg, New York, 2005.
[3] S. Chikazumi, Physics of Ferromagnetism International Series of Monographs on Physics, vol. 94, Oxford University Press, New York, USA, 1997.
[4] V. Skumryev, S. Stoyanov, Y. Zhang, G. Hadjipanayis, D. Givord, J. Nogues, Nature 423 (6942) (2003) 850–853.
[5] M. Rapini, R.A. Dias, B.V. Costa, D.P. Landau, Brazilian Journal of Physics 36 (3A) (2006) 672–675.
[6] M. Rapini, R.A. Dias, B.V. Costa, Physical Review B 75 (1) (2007).
[7] U. Nowak, K.D. Usadel, J. Keller, P. Miltényi, B. Beschoten, G. Güntherodt, Physical Review B 66 (1) (2002) 014430.
[8] D. Lederman, R. Ramírez, M. Kiwi, Physical Review B 70 (18) (2004) 184422.
[9] M. Ali, C.H. Marrows, B.J. Hickey, F. Offi, J. Wang, L.I. Chelaru, M. Kotsugi, W. Kuch, Physical Review B 79 (6) (2009) 064415.
[10] T. Shinjo, T. Okuno, R. Hassdorf, K. Shigeto, T. Ono, Science 289 (5481) (2000) 930–932.
[11] S. Hikami, T. Tsuneto, Progress of Theoretical Physics 63 (2) (1980) 387–401.
[12] S. Takeno, S. Homma, Progress of Theoretical Physics 64 (4) (1980) 1193–1211.
[13] G.M. Wysin, Physical Review B 49 (13) (1994) 8780–8789.
[14] J.E.R. Costa, B.V. Costa, Physical Review B 54 (2) (1996) 994.
[15] J.E.R. Costa, B.V. Costa, D.P. Landau, Physical Review B 57 (18) (1998) 11510–11516.
[16] D. Atkinson, D.A. Allwood, G. Xiong, M.D. Cooke, C.C. Faulkner, R.P. Cowburn, Nature Materials 2 (2) (2003) 85–87.
[17] R.P. Cowburn, Nature Materials 6 (4) (2007) 255–256.
[18] B. Van Waeyenberge, A. Puzic, H. Stoll, K.W. Chou, T. Tyliszczak, R. Hertel, M. Faehnle, H. Brueckl, K. Rott, G. Reiss, I. Neudecker, D. Weiss, C.H. Back, G. Schuetz, Nature 444 (7118) (2006) 461–464.
[19] V.E. Kireev, B.A. Ivanov, Physical Review B 68 (10) (2003).
[20] S.A. Leonel, I.A. Marques, P.Z. Coura, B.V. Costa, Journal of Applied Physics 102 (10) (2007).
[21] J.C.S. Rocha, P.Z. Coura, S.A. Leonel, R.A. Dias, B.V. Costa, Journal of Applied Physics 107 (5) (2010) 053903.
[22] P. Miltényi, M. Gierlings, J. Keller, B. Beschoten, G. Güntherodt, U. Nowak, K.D. Usadel, Physical Review Letters 84 (18) (2000) 4224–4227.
[23] L. Berger, Y. Labaye, M. Tamine, J.M.D. Coey, Physical Review B 77 (10) (2008) 104431.
[24] W.H. Meiklejohn, C.P. Bean, Physical Review 102 (5) (1956) 1413–1414.
[25] W.H. Meiklejohn, C.P. Bean, Physical Review 105 (3) (1957) 904–913.
[26] J. Nogues, I.K. Schuller, Exchange bias, Journal of Magnetism and Magnetic Materials 192 (2) (1999) 203–232.
[27] R.L. Stamps, Journal of Physics D Applied Physics 33 (23) (2000) R247–R268.
[28] M. Kiwi, Journal of Magnetism and Magnetic Materials 234 (3) (2001) 584–595.
[29] J. Nogues, J. Sort, V. Langlais, V. Skumryev, S. Surinach, J.S. Munoz, M.D. Baro, Physics Reports: Review Section of Physics Letters 422 (3) (2005) 65–117.
[30] Ll. Balcells, B. Martinez, O. Iglesias, J.M. Garcia-Martin, A. Cebollada, A. Garcia-Martin, G. Armelles, B. Sepulveda, Y. Alaverdyan, Applied Physics Letters 94 (6) (2009).
[31] O.V. Billoni, F.A. Tamarit, S.A. Cannas, Physica B 384 (1–2) (2006) 184–186.
[32] M. Kiwi, J. Mejía-López, R.D. Portugal, R. Ramirez, Europhysics Letters 48 (5) (1999) 573–579.
[33] R. Morales, Z.-P. Li, J. Olamit, K. Liu, J.M. Alameda, I.K. Schuller, Physical Review Letters 102 (9) (2009) 097201.
[34] J. Eisenmenger, Z.-P. Li, W.A.A. Macedo, I.K. Schuller, Physical Review Letters 94 (5) (2005) 057203.
[35] D. Tripathy, A.O. Adeyeye, Journal of Applied Physics 105 (7) (2009).
[36] S. Prakash, C.L. Henley, Physical Review B 42 (10) (1990) 6574–6589.
[37] A.B. MacIsaac, J.P. Whitehead, K. De'Bell, P.H. Poole, Physical Review Letters 77 (4) (1996) 739–742.
[38] A.B. MacIsaac, K. De'Bell, J.P. Whitehead, Physical Review Letters 80 (3) (1998) 616–619.
[39] E.Y. Vedmedenko, H.P. Oepen, A. Ghazali, J.-C.S. Lévy, J. Kirschner, Physical Review Letters 84 (25) (2000) 5884–5887.
[40] E.Yu. Vedmedenko, A. Ghazali, J.-C.S. Lévy, Physical Review B 59 (5) (1999) 3329–3332.
[41] A. Hucht, K.D. Usadel, Journal of Magnetism and Magnetic Materials 156 (1–3) (1996) 423–424.
[42] D. Toscano, S.A. Leonel, R.A. Dias, P.Z. Coura, J.C.S. Rocha, B.V. Costa, Journal of Applied Physics 109 (1) (2011) 014301.
[43] N.C. Koon, Physical Review Letters 78 (25) (1997) 4865–4868.
[44] M. Kiwi, J. Mejía-López, R.D. Portugal, R. Ramirez, Applied Physics Letters 75 (25) (1999) 3995–3997.
[45] I. Schmid, The Role of Uncompensated Spins in Exchange Biased Systems, Ph.D. Thesis, University of Basel, 2008.
[46] J. Sort, K.S. Buchanan, V. Novosad, A. Hoffmann, G. Salazar-Alvarez, A. Bollero, M.D. Baró, B. Dieny, J. Nogués, Physical Review Letters 97 (6) (2006) 067201.
[47] R.P. Cowburn, Journal of Magnetism and Magnetic Materials 242 (Part 1) (2002) 505–511.
[48] M.H. Qin, X. Chen, J.M. Liu, Physical Review B 80 (22) (2009) 224415.
[49] D.H. Lee, J.D. Joannopoulos, J.W. Negele, D.P. Landau, Physical Review B 33 (1) (1986) 450–475.
[50] J. Nogués, I.K. Schuller, Journal of Magnetism and Magnetic Materials 192 (1998) 203–232.